Robotics Research
Technical Report

ieneratorium omnis laboris ex machina

Area Touch Sensor for
Dextrous Manipulation
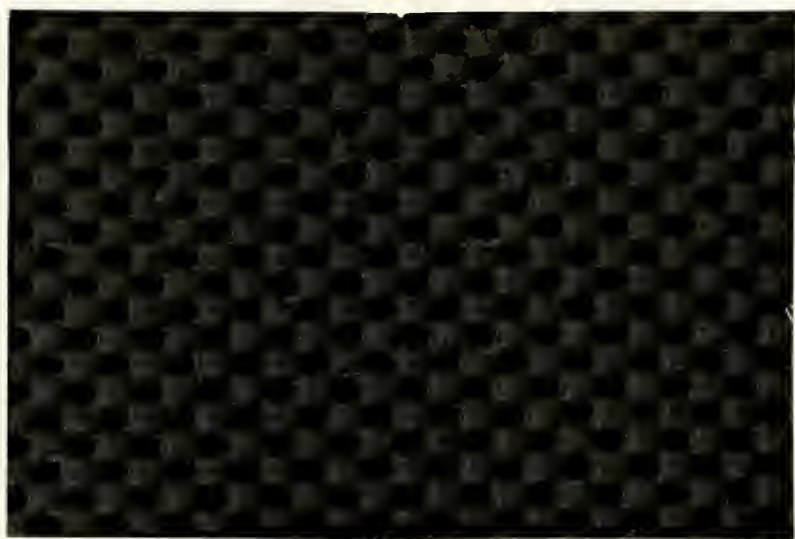
by

C. Marc Bastuscheck

Technical Report No. 388
Robotics Report No. 162
July, 1988

New York University
ant Institute of Mathematical Sciences

Computer Science Division
251 Mercer Street   New York, N.Y. 10012

Area Touch Sensor for
Dextrous Manipulation

by

C. Marc Bastuscheck

Technical Report No. 388
Robotics Report No. 162
July, 1988

New York University
Dept. of Computer Science
Courant Institute of Mathematical Sciences
251 Mercer Street
New York, New York 10012

Area Touch Sensor for Dextrous Manipulation[1]

C. Marc Bastuscheck

Robotics Laboratory
Courant Institute
New York University

ABSTRACT

A touch sensor for robotic applications is described which continuously reports location and magnitude of contact within the active area of the sensor. The thin, flexible sensor may be applied to cylindrical or conical surfaces, and may be made in any nearly rectangular shape and size. A rectangular sensor is explored in considerable detail theoretically. Experiments with several bench-top implementations show excellent agreement with theory, and suggest that devices may be constructed for applications in robotics, orthotics, and prosthetics.

1. Introduction

This paper describes a simple touch sensor which continuously reports position and strength of contact within the area of the sensor. The sensor can take the form of a rectangle of flexible plastic of a size convenient to be used with robot finger elements, although much larger or smaller devices using the principle could be constructed. Prototypes (described below) were sensitive to forces of as little as 2 gms to as much as several kg. This sensor for localization of light touch is intended to work with other sensors such as those for finger position and actuator force, and perhaps vision, to facilitate dextrous manipulation of small objects. Larger versions may find application on the surface of robot arm links or artificial limbs of humans. The sensor requires relatively few wires and only simple electronics. With no multiplexing circuitry, fewer than 60 wires will provide touch sensing for the entire surface of the Utah-MIT hand.

The sensor, sketched in Fig. 1, consists essentially of two thin membranes of conductive material and a means of keeping them electrically separated except when pressure is applied perpendicular to the layers. One of the membranes is kept at some potential V, and electrodes from the four sides of the other membrane lead through current measuring circuitry to ground. When a small force is applied to an area of the sensor the amount of current which flows is primarily a function of contact resistance, and provides some information regarding contact force and area. More important, the distribution of current among the four electrodes gives an excellent measurement of the centroid of a small region of contact and a good estimate of the location of larger irregular contact areas. The localizing capabilities

should be quite similar to those of a tetra-lateral photodiode [W75].

A few working robots are able to sense force on a finger or gripper, and some experimental hands have been equipped with switches or force sensing pads or arrays. Although early force sensing arrays were often rigid and not easily installed in robot fingers, this is changing (see section 2). However, if the entire surface of a robot hand is to be covered with a mesh of small sensing elements it is clear that problems in communications and quantity of data arise [Jea88]. A different approach is suggested in this paper. It is assumed that the primary function of tactile sensors is to report contact of a portion of the robot hand with an object, and that only a rough idea of contact magnitude and location is required. Consider, e.g., groping for a cup, or rotating a pen in the fingers, tasks in which a tactile sense should report even very light touches but ignore fine detail. These tasks require only information which could be generated by the sensor described here. There are of course tasks requiring fine detail, and for these different sensors might be installed on one or two finger tips. However, simple, economical sensors can probably handle many tasks. The primary motivation for this paper is the introduction of a relatively simple touch sensor with which to approach experimentally interesting issues of manipulation.

The paper is organized as follows: section 2 explores the nature of tactile sensing. Section 3 describes the new sensor mathematically to clarify the interaction of important parameters such as size, shape, force, contact area, and resistances. Experiments which demonstrate the potential of the device and support the theory are described in section 4. Problems of manufacture, installation, and use are considered in section 5, where related sensors are also briefly described.

2. Short Summary of Tactile Sensing

Human tactile sensations include perceptions such as object location, shape, hardness, temperature, texture, thermal conductivity, wetness, and many more; interpretation of sensor input is prominent in most of these. Robot tactile sensation is far more limited, not to say non-existent, and is usually only raw transducer output. There is little agreement of what sensors should be, what they should record, or what can be done with the information. The state of the art has changed very little since the description by Harmon [Ha82], due to difficulty in producing adequate sensors, lack of sufficiently dextrous robots, and lack of understanding of needed higher level processes. A thorough review of early tactile sensing work is [H80], and a flavor of current research can be found in [DD85].

2.1. Biological Sensing

Robotic tactile sensing should not necessarily be modeled on biological sensing, since the transducers, signal conduction media, and signal processing topologies are very different in the two systems. However, the basic problem is similar in both cases, and results from investigations of working tactile sensing systems should not be entirely ignored. No biological system is well understood, despite considerable study. However, the following observations of the human tactile system are generally accepted [G78].

- 2 -

The human sense of touch utilizes several different types of sensors, including "rapidly adapting" sensors which respond only to changing mechanical deformation of the skin, "slowly adapting" sensors which respond even to static mechanical deformation (although the brain tends to ignore dc signals), sensors for heat, for cold, and for large stimuli (mechanical or thermal). The human sensory system appears to be similar to that of other animals, and many experiments done with cats and monkeys provide information relevant to the human system; these experiments have made it possible to correlate identifiable anatomical structures with low-level sensing functions. The visco-elastic properties of the skin and its ridged structure both seem to be very important, but exact mechanisms are not yet entirely understood. Threshold of sensitivity to small contacts can be as small as 0.03 gms force for "rapidly adapting" sensors, and 0.6 gms force for slowly adapting sensors, but the thresholds depend on the location of the stimulus with respect to a sensing cell (threshold can vary by a factor of 20) and by the individual sensor. Large forces are sensed by large threshold cutaneous sensors (nociceptive units), and by sensors in the muscles, tendons, and joints. Although some sensors report muscle/tendon tension directly, it appears that the effort commanded by the brain to be expended in performing a particular task is a more important measure of force: an object appears to be heavier when the muscles are fatigued.

Some local processing of signals, such as inhibition of a sensing cell by its neighbors, is likely, but far less processing takes place than in the retina of the eye. Specialized sensitivities, such as signals in response to a particular motion across the surface of the skin, have been reported, but it is not known if such signals come from special sensing cells or from local processing. Different regions of the skin show different absolute and relative densities of the various types of sensing cells, resulting in different capabilities and acuities in different body regions. In some regions of the skin no more than 0.2 mm separates sensors of a particular type, but spacing of several millimeters is more common. Experiments have shown that sensing systems become less sensitive just before and during active motion.

An extremely important observation relevant to the design of robot sensing systems is that *effective object recognition by humans requires active touch*. "Active touch" means that the subject is allowed to manipulate an object or move his/her fingers over an object. Another observation, a speculation from the study of the origins of man, may be worth considering: manufacture and use of tools is claimed to have occurred at the same time that fleshy fingerpads developed. (Modern apes and chimpanzees do not have fleshy fingerpads.) There is also theoretical support for using something like a fleshy contact during grasping [B84].

2.2. Machine Sensing

A large number of physical processes can be used to transform force or mechanical deformation into an electrical signal. However, it is difficult to take any physical process and develop a robust, reliable, and cheap sensor with large signal, low noise, good linearity, low hysteresis, and suitable mechanical properties. Most attention has been given to developing arrays of sensors so fine details of a surface can be perceived and parts discriminated by touch; this means that sensing elements must be small and increases the possibility of crosstalk between adjacent sensors. It also means that many wires must be used, or some means of multiplexing signals be

provided.

The simplest sensors which provide more than on/off information consist of contact with or between conducting elastomers [SS78] [Hi82] [RT82] [RW83]. Conducting elastomers are not ideal, but their tendency to degrade with time and use may have been overcome in a new force sensitive resistive (FSR) material [IE]. This is available as a thin film in the form of arrays even in a "potentiometer", which allows one, with suitably clocked connections, to determine both location (in one dimension) and strength of contact. Tise [T88] has developed a 0.5x0.5x0.25 inch sensor package which contains a 16x16 contact array on its surface and complete multiplexing and a/d circuitry inside using FSR material with which he has recorded 10 tactile images per second. The sensor is as yet not robust, and is limited by the FSR material to forces over about 30 gms per element.

Two sensors have been developed using arrays of capacitors inside elastic finger structures. Fearing and Binford [BF88] report a mean sensitivity of 0.4 gms but could not make measurements to determine the radii of contacted cylinders with less than 50 gms applied force; the MIT sensor [SGH86] - which incorporates both mechanical and thermal sensors - works in the range of 0 to 200 gms with considerable hysteresis and resolution of 5 - 10 gms.

Another finger incorporates an array of 256 optic fibers arranged to collect light as a function of force applied over the end of each fiber [B88]. (References to other sensors based on optic fibers can be found there.) Although a force range of 0 to 40 gms per element is claimed, images showing recognition applications were made with forces of 4 to 5 kg, suggesting that the present sensor is relatively insensitive to small forces. Yet another finger has been developed using ferroelectric polymers to make a skin-like tactile sensor [Dea85].

The tactile sensor described in this paper has apparently not been previously published. It should be valuable in providing a sense of light touch over many areas quite cheaply. It will work well in a complex environment such as that of the Utah-MIT hand, where joint position and tendon tensions are known, one or two high resolution finger-tip sensors may be present, and vision may be available.

3. Theory

The sensor can be thought of as two parallel planar conductors, sketched in fig. 1. Without loss of generality the upper plane can be considered to have good conductivity, while the lower plane has resistance of ρ/w ohms per square. The upper plane is held at voltage V, and the edges of the lower plane are held at ground potential. Excellent conductors, along the edges of the lower membrane but not quite touching at the corners, collect current from each of the four sides for measurement. When pressure is applied to a point on the upper plane it deforms and causes a small region of electrical contact between the two planes, allowing current to flow. It will be shown, in section 3.1, that that the location of a point contact can be determined unambiguously from the distribution of current collected by the side electrodes. In section 3.2 a model is investigated to determine how the total current might be expected to depend on area of contact, contact pressure, contact resistance, and resistance of the lower plane from the contact area to ground. In section 3.3

several extensions of these results are considered, including observation of non-point contacts and design of related sensors.

3.1. Location of a Point Source

The flow of current through a thin, rectangular conductor from a point source is considered with a view toward determining the location of the source within the rectangle; the upper conducting plane is ignored for the moment because it merely serves to bring current to the contact region. This is a specific simplification of the general problem of current (or heat) flow, and solutions are well known. A complete derivation of this particular solution is, however, given in appendix A. It will be shown that the location of a point source can be determined by measuring the currents collected at the four sides of the rectangle.

Current, flowing in the plane, follows the gradient of the electric potential U, which itself is a solution of the two dimensional Poisson equation

$$\nabla^2 U(x,y) = \frac{\partial^2 U}{\partial x^2} + \frac{\partial^2 U}{\partial y^2} = -\frac{\rho}{w} J(x,y) , \tag{1}$$

where ρ is the resistivity of the material, w is the thickness of the plane, and $J(x,y)$ is a spatially varying current source. The contact area can be modeled as a point source at (x_0, y_0) by using Dirac delta functions: $J(x,y) = J_0 \delta(x - x_0)\delta(y - y_0)$. If the resistive plane occupies the rectangular region $0 \le x \le a$ and $0 \le y \le b$ the potential can be written as the Fourier expansion

$$U(x,y) = \frac{4\rho J_0}{\pi^2 abw} \sum_{m=1}^{\infty} \sum_{n=1}^{\infty} \left(\frac{m^2}{a^2} + \frac{n^2}{b^2} \right)^{-1} \sin\frac{m\pi x_0}{a} \sin\frac{n\pi y_0}{b} \sin\frac{m\pi x}{a} \sin\frac{n\pi y}{b} . \tag{2}$$

The current exiting a side is determined by noting that the potential difference across an infinitesimal element is both the gradient of the potential at that element and the product of the resistance of the element and the current traversing it. Carrying out algebra for the current which leaves the side at $x = 0$ yields

$$I_{x=0} = \frac{8J_0}{ab\pi^2} \sum_{m=1}^{\infty} \sum_{n=1}^{\infty} \frac{\dfrac{m}{2n-1}\dfrac{b}{a}}{\left(\dfrac{m^2}{a^2} + \dfrac{(2n-1)^2}{b^2} \right)} \sin\frac{m\pi x_0}{a} \sin\frac{(2n-1)\pi y_0}{b} . \tag{3}$$

Although the sums in eq. 2 need not be extended to infinity, n and m must both go to several hundred for reasonable accuracy. To reduce computation time this double sum can be reduced to a single sum [J61], leading to

$$I_{x=0} = \frac{4J_0}{\pi} \sum_{n=1}^{\infty} \frac{\sin[(2n-1)\pi y_0/b]}{2n-1} \frac{\sinh[(2n-1)\pi(a-x_0)/b]}{\sinh[(2n-1)\pi a/b]} . \tag{4}$$

Currents for the side at $x = a$ can be written down immediately using symmetry from eq. 4:

$$I_{x=a} = \frac{4J_0}{\pi} \sum_{n=1}^{\infty} \frac{\sin[(2n-1)\pi y_0/b]}{2n-1} \frac{\sinh[(2n-1)\pi x_0/b]}{\sinh[(2n-1)\pi a/b]} , \tag{5}$$

and similar equations result for the top and bottom currents by interchanging a and b, m and n, and x and y. Currents computed using these expressions converge very

rapidly; summing only the first 10 terms yielded a total current within 0.01% of J_0 for x and y values between 0.1 and 0.9 of full scale.

For sensing purposes it is necessary to invert eqs. 4 and 5, i.e. to determine the source location as a function of observed currents. This cannot be done exactly. However, the dominant behavior of the currents as a function of source location can be observed by re-writing $2\sinh\theta$ as $e^{\theta}-e^{-\theta}$ and neglecting $e^{-\theta}$ as being relatively small. (The effect of these approximations, which are used only to discover a quantity for measurement, is small except near the sensor boundaries.) This leads to

$$I_{x=a} \approx \frac{4J_0}{\pi} e^{-\pi(a-x_0)/b} \left[\sin\pi y_0/b + \frac{e^{-2\pi(a-x_0)/b}\sin 3\pi y_0/b}{3} + \cdots \right] \qquad (6)$$

with a similar expression for $I_{x=0}$. The ratio of currents from opposite sides can be approximated as

$$\frac{I_{x=a}}{I_{x=0}} \approx \frac{e^{-\pi(a-x_0)/b}}{e^{-\pi x_0/b}} = e^{2\pi(x_0-a/2)/b}. \qquad (7)$$

This suggests that an "observed" position can be defined as

$$x_{obs} = \frac{a}{2} + \frac{b}{2\pi} \log\frac{I_{x=a}}{I_{x=0}} \qquad (8)$$

$$y_{obs} = \frac{b}{2} + \frac{a}{2\pi} \log\frac{I_{y=b}}{I_{y=0}}.$$

(Here, and throughout this paper, natural logarithms are used.) The dependence of x_{obs} on x_0 is plotted in Fig. 2 for several values of y_0, where I values were generated by summing eqs. 4 and 5 numerically. The approximations made in deriving eqs. 6 and 7 show up as deviations from the straight (dashed) line in Fig. 2. The value of x_{obs} and y_{obs} is that they are easily computed from observed currents, and can be related to the true source location (x_0,y_0) using a function or look-up table to approximate the curves of Fig. 2. For some work, however, approximate locations may be adequate, and constants a and b in eq. 8 can be adjusted so the "observed" position is close to the true position with error spread over the surface of the sensor. Fig. 3 shows such observed positions displaced from their true positions for one choice of proportionality constants.

In this section it has been shown that the location of a point contact can be determined using the integrated current flow to the four sides. It is shown in section 3.3 that this result holds also for small and even extended regions of contact. It may be possible to determine the shape of an extended source under some circumstances.

3.2. Contact resistance and total current flow

Information made available by the sensor concerning the location of contact is independent of the absolute strength of the total current. It should be possible to extract information concerning strength of contact from the size of the current, since the sum of the currents is inversely proportional to the sum of the contact resistance and the effective resistance of the planar conductor. A method for estimating the resistance of the planar conductor is given, then current flow from an electrode into

a conducting plane through a resistive layer will be considered in sufficient detail to produce a useful mathematical model of the process.

It appears trivial to determine the resistance presented by the plane to a point source of current. Simply setting $x = x_0$ and $y = y_0$ in eq. 2 gives the potential, and dividing this by J_0 defines the resistance of the plane from Ohm's law. Unfortunately, this results in an infinite resistance, due to the assumption of a truly point source. Truncating the sums at some limiting index value corresponds to broadening the contact "point", since terms in the potential which would change magnitude significantly over the contact region are excluded (on the very reasonable ground that they cannot contribute). Relevant experimental observations are discussed in section 4.1. For small contacts the resistance is found to change slowly except near the edges, and can be considered roughly constant. For accurate work specially constructed look-up tables may be useful. In the following model the resistance of the plane is calculated in a different manner, strictly valid only for centered contacts, but the above argument shows that the value obtained is good over much of the sensor area for small contact regions.

Since most regions of contact will be, to a first approximation, circular, and since details of the edge geometry are negligible when the region of contact is not close to an edge, a cylindrical geometry is used in this investigation of current flow into a planar conductor. Consider a rod of high conductivity held at potential V^+ which is pressed against the center of a circular planar resistor. The rod has radius A, the planar resistor has radius B, resistivity ρ, and thickness w (thus ρ/w ohms/square), and its circumference is held at potential 0 (ground). Current from the cylindrical electrode passes through a uniform (surface) resistive layer of $\sigma/\pi A^2$ ohms.

From symmetry, current flows radially within the plane, and current at $r = 0$ is zero. Let $I(r)$ represent the current crossing a cylindrical surface at radius r. For $r < A$, as r increases $I(r)$ increases, the rate depending on the contact resistance between the electrode and the planar conductor, and the resistance of the planar conductor. $I(r)$ is constant for $r > A$, since there are no current sources or sinks until $r = B$. Intuitively, if the contact resistance is very high, current will flow nearly uniformly through the end of the rod, while if the contact resistance is very low current will enter the planar conductor primarily along the outer edges of the rod.

Detailed consideration (appendix A) allows a functional form for $I(r)$ to be determined:

$$I(r) = a_2 \sum_{m=1}^{\infty} \left[\frac{\rho A^2}{4w\sigma} \right]^{m-1} \frac{1}{m!(m-1)!} \left[\frac{r}{A} \right]^{2m}, \qquad (9)$$

where

$$a_2 = \frac{V^+}{\dfrac{\sigma}{\pi A^2} + \dfrac{\rho}{4\pi w} \sum_{m=1}^{\infty} \left[\dfrac{\rho A^2}{4w\sigma} \right]^{m-1} \dfrac{[2\log(B/A) + 1/m]}{m!(m-1)!}}. \qquad (10)$$

The factor $\dfrac{\rho A^2}{4w\sigma} \equiv r_R$, very important in determining the character of $I(r)$, is best understood as the ratio (within a constant) of the resistance of the resistive

plane to the contact resistance between the rod and the plane. When $r_R < 1$, i.e. contact resistance relatively large, only the first term ($m = 1$) is significant. When $r_R \gg 1$ the greatest contribution to the sum occurs for $r_R = m(m+1)$. (This follows from setting the derivative with respect to m of $\dfrac{r_R^{m-1}}{m!(m-1)!}$ equal to zero, writing $m!$ as $\Gamma(m+1)$, and using Stirling's formula $\Gamma(x) \approx e^{-x} x^{x-1/2} (2\pi)^{\frac{1}{2}} (1 + \text{correction terms})$.) Although several values of m about $m = \dfrac{1}{2}(\sqrt{4r_R+1}-1)$ contribute strongly to the sum, the behavior of $I(r)$ under the electrode can be most easily understood by thinking of $I(r)$ as proportional to $(r/A)^{\sqrt{r_R}}$. When r_R is large, current flows into the conducting plane only near the edges of the electrode, while for small r_R current flows nearly uniformly across the contact surface.

The total current is, from eqs. 9 and 10,

$$I(A) = \frac{V^+ \sum\limits_{m=1}^{\infty} \left[\dfrac{\rho A^2}{4w\sigma}\right]^{m-1} \dfrac{1}{m!(m-1)!}}{\dfrac{\sigma}{\pi A^2} + \dfrac{\rho}{4\pi w} \sum\limits_{m=1}^{\infty} \left[\dfrac{\rho A^2}{4w\sigma}\right]^{m-1} \dfrac{[2\log(B/A)+1/m]}{m!(m-1)!}}. \tag{11}$$

If the contact resistance is independent of force, for very small areas the contact resistance is far larger than the resistance of the plane, and only the $m = 1$ term contributes to the sum. $I(A)$ increases with increasing area until the contact resistance $\sigma/(\pi A^2)$ becomes comparable to ρ/w. With further increase in area $I(A)$ increases more slowly, and with further increase of area becomes nearly constant unless the area of contact approaches the size of the plane. Typical behavior is shown in Fig. 4; note the unit slope at the left side showing that the current is proportional to the contact area.

It is far more common that contact resistance is a function of pressure than otherwise. Possible mechanisms include deformation of surface micro-structures to change contact area on the microscopic scale, changing conductivity of surface layers at microscopic points of high pressure, deformation of resistive polymers (which typically consist of an insulating plastic material containing particles of a conductive substance such as silver or carbon black) to bring conducting particles into contact, etc. These effects may occur simultaneously and are extremely difficult to analyze experimentally. However, the net effect is often simply that the contact resistance varies as some power of the applied pressure:

$$\sigma = \frac{k}{(F/\pi A^2)^\alpha} \tag{12}$$

where pressure is represented as a force F divided by area. In this form current increases with increasing force if $\alpha > 0$.

$I(A)$ vs pressure (or, equivalently, force) was plotted for a number of values of ρ/w, k, and A using eqs. 11 and 12. The behavior was quite simple: at low forces (pressures) the current increased as F^α; at intermediate forces $I(A)$ increased more slowly, and at high forces $I(A)$ did not change. Fig. 5 plots current vs. force for $\alpha = 1.5$. The distinction between low, intermediate, and high forces is determined by the choice of materials. However, it appears to be relatively easy to work in the

low force region (see experimental section). In this case

$$I(A) \approx \frac{V^+}{\dfrac{k}{\pi A^2}\left[\dfrac{\pi A^2}{F}\right]^\alpha + \dfrac{\rho}{4\pi w}(2\log B/A + 1)} \,. \tag{13}$$

Generally it is difficult to separate the effects of force and area. However, for $\alpha = 1$ in the small force limit the area divides out, and $I(A) = V^+ F/k$, independent of contact area. Thus if only force is desired, materials should be chosen which produce $\alpha = 1$. Combining such a sensor in a sandwich with another having a different α should make both force and area of contact measurable.

3.3. Extensions and related problems

In section 3.1 it was shown that the location of a point contact within a conducting rectangle could be determined by measuring total currents flowing to the sides. There are many related mathematical problems, solutions for which may be relevant to this tactile sensing problem.

Some extensions are trivial. In section 3.1 time dependence was ignored - quite properly since electrical signals propagate very quickly (at the speed of light) compared to relevant mechanical motions of the sensor. (The situation is different with tetra-lateral photodiodes and detectors used in high energy physics, where carrier mobility sets signal propagation times and signal rates may be quite high.) It was assumed that the resistance of the plane was isotropic; this could be trivially relaxed to allow anisotropic conductivity by rescaling distance variables appropriately, and could be usefully exploited to make a long rectangular sensor (perhaps wrapped around a robot finger) seem square. Mapping a planar sensor onto a ruled surface (cylinder, prism, cone) does not affect the mathematics.

If the sensor were limited to point contacts it would not be very useful. However, solutions to eq. 1 can be superposed: if two point contacts are present the solution U and the currents are simply the sum of the solutions for the contacts made separately, and this argument can be extended to show that solutions exist for any area of contact. For small areas of contact the position returned by the method of section 3.1 gives a very good approximation to the center of the region of contact (next paragraph). If all contacts are not equally weighted the resulting average point of contact will be closer to the points contributing more current, a desirable result.

Consider two point contacts at $x = 0.5$ and $x = 0.7$ on the y midline of a unit square sensor, both injecting $J_0/2$. The side currents, in units of J_0 for this case are $I_{x=1} = 0.359$ and $I_{x=0} = 0.185$, with $I_{y=0,1} = 0.228$, yielding $x_{obs} = 0.606$ from eq. 8. This is very close to $x_{obs} = 0.608$ for a point contact at $x = 0.6$, i.e. the average point location is returned with negligible error. However, in addition to providing a useful average point of contact, the information returned by the sensor can indicate that the observed contact is elongated parallel to one of the axes. For a point contact at $x = .6$ the ratio

$$\frac{I_{x=1} + I_{x=0}}{I_{y=1} + I_{y=0}} = \frac{0.522}{0.478} = 1.09 \tag{14}$$

while for point contacts at .5 and .7

$$\frac{I_{x=1} + I_{x=0}}{I_{y=1} + I_{y=0}} = \frac{0.544}{0.456} = 1.19 \ . \tag{15}$$

Thus a quick check of (total x current)/(total y current) shows that the observed contact is not a point contact, and indicates direction of elongation.

This leads to the mathematically interesting question: how much information about the contact region can be derived from currents measured at the boundary of the sensor? This type of "inverse" problem presently receives much attention [K88] because in many applications (geology, engine design, solar physics) questions are posed in the form of "given a few measurements on a bounding region, what is going on inside?". As a practical matter, would it make sense to divide the edges of the detector into additional separate measuring regions? It is well known that even with complete knowledge of the current flow at every point on the edges additional constraints on the source are required to provide a unique solution [C75], and this can be shown using a simple argument. Consider a single point contact which sets up the potential of eq. 2. Along an arbitrary equipotential line on the surface of conductive area paint a very thin conducting stripe; this will change nothing in the boundary currents. Connect a battery to provide the observed potential to this conducting stripe (again, nothing changes). Now, however, the original point contact could be removed, or the region bounded by the equipotential stripe could be filled with conducting paint and no change would be observed at the boundary. (This assumes that surface contact resistance is negligible.)

Other mathematical problems also arise. In section 3.1 it was assumed that the boundary was held at ground potential (zero Dirichlet conditions), and this greatly simplified the solution. It does not make sense to use zero Neumann boundary conditions (no current flow out of the sides) on all sides, but information might be obtained using mixed boundary conditions. Experimentally it may be convenient (section 4.2) to place resistors between the electrodes and ground, a condition for which analytic solutions do not exist, but which are physically well defined. What information might be obtained if each side were divided into n segments and the current from each segment could be individually switched to pass directly to ground or pass through a resistor to ground? Such an arrangement provides 4×2^n different measuring conditions with no moving parts. How much more information is available as n increases?

Another area of practical importance might be investigated, namely, the shape of the sensor. Solution for a rectangle is relatively simple, but arbitrary polygonal or curved boundaries also provide stable potential distributions and may generate useful sensor configurations. Slight changes in electrode shape (or variation in the conductivity of the plane, though this may be difficult to fabricate) might provide more linear response of the sensor output to position. Geometry other than planar may have to be studied, since a spherical (or other) surface is needed to make a fingertip sensor.

4. Experiments

Experiments were carried out to determine if practical devices could be made which would show behavior expected from section 3. These included 1) measurements of currents collected at the sides of a square of conducting plastic as a function of the location of electrical contact within the square; 2) investigations of current as a function of force and area for objects pressed against a couple of two-layer devices of a size which might be used on a robot finger element; and 3) trials extended in time to investigate stability.

4.1. Simple test with computer sensing

A feasibility test was carried out using two pieces of conducting foam separated by a coarse plastic mesh. A potential of 6V was applied to the upper plane, and metal electrodes clamped to the edges of the lower plane collected currents, which flowed through 100 Ω resistors to ground. Voltages across the four resistors were measured using a Data Translation A/D board in an IBM PC. Position of touch was indicated graphically within a rectangle on the screen of the PC using eq. 8, and the sum of the logs of the currents was displayed as an indication of contact force. The crude device tracked position within about 10%, and responded with larger numbers as the force of contact increased. Resolution was limited by the plastic mesh and by the approximation used to compute logarithms.

4.2. Accurate measurement of current vs. position

A large square, 13.2 cm on a side, of 0.005 inch thick carbon black loaded conducting polymer ($\approx 2.4 k\Omega$/square) was used to measure side currents as a function of contact location. An electrode was formed along each side by applying a strip of silver paint about 3 mm wide to within 7mm of the ends, holding a fine wire along each side with a strip of aluminum foil folded around the edge of the plastic, and anchoring the whole with Scotch tape. The fine wires extended several inches away from the square for easy electrical connection. The area between the electrodes was about 12.5 cm square. A banana plug, held at 6V potential, was pressed firmly and perpendicularly against the plastic at a number of points along the centerline of the square, and also along a line parallel to the center. Currents from top, bottom and left side were measured using digital Fluke multimeters. The current from the right side was not measured, and passed directly to ground.

The current to each side was about 0.6 ma when the contact was in the center, and the "top" current varied from less than 0.10 ma to over 3.0 ma as the contact point was moved from bottom to top. Measurements spanned 11 cm about the center of the sensor. Data from one set of measurements is shown in Fig. 6, where $\frac{1}{2\pi} \log(I_{top}/I_{bottom})$ is graphed against displacement of the contact point across the sensor. Vertical and horizontal scales for data points (circles) and the solid theoretical curve are absolute; the horizontal offset of the measured locations was chosen to fit the data because the center position was not accurately recorded during data taking. Measured points agreed very well with theory.

As shown in fig. 6, the log of the ratio of the currents is close to linear in position over much of the sensor area. (The dashed line in fig. 6 represents linear behavior, which, of course, is not theoretically correct.) The sensor response can

be made more linear by adding a resistor between each current collecting electrode and ground; however, this reduces the size of the currents, and thus the sensitivity of the sensor. Adding a 336 Ω resistor to each side reduced the deviation from linearity by about a factor of 3, and reduced the currents by a factor of about 2.

On the basis of these experiments it appears possible to locate a small region of contact to within about 0.2 cm in the 12 cm square, not counting the expected systematic deviation from linearity. The sensor might be better than this, since there was uncertainty in positioning the banana plug (about 1 mm), and error in reading the currents, which changed slightly in time (perhaps due to small changes in contact force) and could not be read exactly simultaneously. This problem was only one of simultaneous recording, since observed location is entirely independent of the size of the currents, and thus of the applied force. The systematic deviations from linearity can be corrected, since the form of the deviation is known theoretically. Performance of the sensor would be limited by local variation in resistivity, by inaccuracies in dimension or electrode geometry, and by impedance and resolution of measuring equipment.

With sufficient force applied the currents changed very little, and it appeared that the contact resistance was, if not negligible, at least changing very slowly with force. (Direct measurements of the contact resistance using a multimeter were inconclusive.) Thus a measure of the variation of resistance of the plane with contact location could be made by defining this resistance simply as the applied voltage divided by the total current flowing to all four sides. The current flowing to the right side was assumed from symmetry to equal that to the left.

Fig. 7 shows resistance vs position for the measurements of fig. 6. The theoretical curve changes shape depending on the number of terms summed in determining the potential $U(x,y)$ (eq. 2). More terms correspond to a better approximation of a true point contact; summing m and n to infinity would produce a resistance independent of position, but physically meaningless. Lower limits on summing indices result in rounded shapes, as in fig. 7, with shape changing relatively slowly with the summing limits. A limiting index m_{lim} for the sums can be estimated by assuming that it makes no sense to consider contributions to the potential which change significantly over the area of contact, i.e. $m_{lim}\pi\delta x/a$ should be a fraction of π. Assuming $m_{lim}\delta x/a = 1/4$, and using $a = 12.5$ cm and $\delta x = 0.05$ cm (approximate radius of contact region of spherical end of the banana plug), yields $m_{lim} \approx 60$. This is a crude estimate, and δx could just as easily be taken to represent the diameter of contact area instead of radius, giving $m_{lim} \approx 30$.

The solid curve in fig. 7 was generated using $m_{lim} = 45$, which fit quite well, but was slightly below the data points closer to the edges. Adding a contact resistance of 0.2 $k\Omega$ to the theoretical values for the resistance of the plane improved the fit, and this is the theoretical curve in fig. 7. A curve generated using $m_{lim} = 531$ clearly did not fall off sufficiently quickly away from the center. These values for m_{lim} and the contact resistance seem reasonable in the context of all experiments.

4.3. Dependence of Current on Force and Area

A prototype sensor (S1) 6.2 cm long and 3.5 cm wide was constructed using two sheets of this same conducting plastic. Electrodes were applied to the edges of the lower plane in the same manner as to the large square of section 3.2, except

thinner strips of silver paint were applied to the edges and smaller gaps of about 2 mm were left at the corners. The second layer of plastic was placed immediately above the bottom plane, and a layer of aluminum foil with a fine wire attached was placed above this to avoid resistive losses in the upper plastic plane. With no applied force no current (or very little) flowed between the plastic planes.

Experiments consisted of placing various objects near the middle of the sensor surface and recording the currents from the narrow ends using digital Fluke multimeters. Currents from the broad sides, not measured, went through 336 Ω resistors to ground to increase current flow to the end electrodes. Objects included spherical knobs of three sizes which were used with both round side and flat side down, and a thin plastic spacer about 1 cm square which had rounded corners and 4 2.5 mm diameter interior holes. A potential of 12 volts was applied to the upper plane, producing currents to each end of up to several ma. Different forces were applied by placing known masses (brass weights) on these objects. Forces are recorded here using the unit "gram-force" (gf), i.e. the weight of the corresponding mass in grams. One newton = 102 gf.

The general nature of the results of this section can be understood by rewriting eq. 13, valid for low pressure, as

$$I = \frac{V}{R_c + R'_p} , \qquad (16)$$

where the contact resistance R_c varies inversely with pressure, resistance of the plane R'_p is determined by the size and location of contact area, V is the applied voltage and I is the measured total current. Pressure is merely the applied force divided by the contact area, so high pressure can be obtained by using a large force on a moderate area or a moderate force on a small area.

Fig. 8 shows observed currents vs. force plots for two objects. The most complete current vs. force information was obtained using the plastic spacer, primarily because measurements could be made at very low forces and pressures. Measurements below 2 gf produced currents below the resolution of the Fluke multimeters. Current increased as force increased in a manner very similar to the theoretical curve in fig. 5. For the plastic spacer, the transition from contact-limited current at low force to current limited by plane resistance at higher forces is clearly seen. For the small sphere only the high pressure end of the theoretical curve was accessible in this experiment because the sphere had a mass of 10 gms and a small contact area. At large pressures the current is determined entirely by R'_p.

If R'_p is kept constant by keeping the contact area and position fixed for a series of different forces, the dependence of R_c on force can be determined. Then, if R_c is inversely proportional to F^α, α can be determined from a log-log plot of $R_c = V/I(F) - R'_p$ vs F. An initial estimate of R'_p can be made from the large force current, and this value can be refined to produce a straight line of $\log(R_c)$ vs $\log(F)$. This analysis was carried out for the spacer and for the three knobs, with both spherical and flat sides against the sensor. When flat sides were against the sensor the exponent α was found to be 1.5 $\pm$.1. When the round side was against the sensor this analysis suggested variable α - as might be expected if contact area and force were changing. Unfortunately the range of data was insufficient to verify this.

Observed values for the resistance of the plane generally scaled with the contact dimensions according to the $\log(B/A)$ relation of eq. A29. However, exact verification was difficult because the sensor was rectangular, its long sides were not held at zero potential, the current from the long sides was not measured, and the areas of the experimental objects were poorly defined, having holes and other surface irregularities.

A second sensor (S2) was constructed from a 6.2 x 3.5 cm strip of a different conducting polymer [3M] which was thinner (0.004 inch) and more resistive ($\approx 15k\Omega$/square). Electrodes were formed as before (silver paint, aluminum foil, and fine wire leads) in S2; however, aluminum foil alone was used as the upper membrane. Position of touch was reliably sensed, with data similar in shape to the curves in Fig. 2. Because of the greater resistivity forces smaller than 5 gf could not be observed with 12 volts applied. Most current change with increasing force occurred below 150 gms, but the current continued to increase slowly with applied force even up to forces of several kg.

4.4. Extended Observations

To investigate stability of measurements over long time periods and under varying conditions a device was constructed to raise and lower a weight onto the sensor repeatedly. A weight of 300 gms pressed primarily vertically against the plastic spacer, which was taped to the table to reduce horizontal motion and keep the contact in the same location on the sensor. Both sensors were tested, with approximately 8300 repetitions for S1 and 10300 for S2 at a rate of 6/min. At any time the total current flow could be measured using the arrangement shown in fig. 9. After all trials measurements of current vs force were repeated (as in fig. 8) with results very similar to the initial results, although the low force currents were more erratic. In the case of S1 these second measurements were made 8 weeks after the initial measurements, and no special care had been taken in the storage of the sensor during that time.

Response of both sensors was similar: current flowed with weight on, and ceased when the weight was removed. Current dropped abruptly as the weight was removed, but increased with a slight delay, reaching full value about 1 sec after the weight was in place. The peak value of current varied randomly by about 5%, and successive peak values decayed in time. Removing the potential for several hours caused the peak value to return to its original value. The behavior for the two sensors differed in detail: for S1 the signal decayed to zero, while for S2 it remained at about one fourth its original value for long periods of time; for S1 the decay time decreased as the mechanical cycling progressed while for S2 leaving the potential off for 10 hours restored the sensor to its original state.

The observed peak signal for both sensors depended on the history of application of potential and of weights. For example, when S1 showed no current during repeated application of 300 gms, applying an extra 200 gms gave exactly the signal expected for 200 gms (and this also decayed); removing the 200 gm weight caused currents to be observed again for the 300 gms. At times there was also a sensitivity to thermal changes in the area. These particular sensors would work poorly in a repetitive task, but might be useful with a variety of forces and contact locations. Location of contact can be determined even when magnitude of contact is not

entirely known.

4.5. Summary of experimental observations

It has been demonstrated that an area touch sensor, suitable for bench-top measurements, can be constructed relatively easily from available materials. The sensors were able to give locations to within the accuracy of measurement ($\approx 2\%$) for small regions of contact, and some indication of strength of contact. A significant feature of these sensors is the useful response at very small forces - the 10 gm sphere with no added weight generated a total current which was 20% of the largest current observed in the course of the experiments. However, in these implementations effects of area and pressure together contributed to the total current. In actual implementations additional information (e.g. from tendon force sensors, vision data, or object continuity) may be available to reduce ambiguity. Intelligent use of an area touch sensor should include recording responses to slight finger motions such as squeezing an object, which would distinguish between the two curves in Fig. 8 if an independent (crude) measure of force were available.

The experiments were not designed to test the theoretical results of section 2 precisely. However, the experimental observations are consistent with theoretical behavior in all important areas: 1) dependence of contact position with log of ratio of currents to opposite sides; 2) variation of resistance of the plane with contact area; and 3) variation of resistance of the plane with contact location. Within the limits of experimental accuracy quantitative agreement with theory was excellent. In addition, the assumption of a simple exponential law for current vs. contact force appears to hold for these materials.

Mechanical cycling did not lead to simple failure of the sensors tested, but repeated application of a known force did not produce repeated identical output currents. Regular behavior was observed, but this was regularity in the rate of change of the measured peak currents, which appeared to depend on the history of application of potential and history of application of force. Application of a variety of weights, as in the tests of section 4.2, seemed to restore each sensor to its initial condition.

5. Further Work

Area tactile sensors such as those described above can be used to report the location and magnitude of touch. One would like to jump from these experimental and theoretical results directly to the ideal implementation in which the Utah-MIT hand effortlessly picks up a bolt and adjusts the orientation so the end without the head can be started in a hole, using tactile sensors which are not apparent to a casual glance. Such an implementation appears possible, but considerable work must be done to establish this, let alone implement it. In particular, the nature of tactile sensing and active touch must be carefully considered, sensors must still be developed, issues of manufacture, installation and data communication must be addressed, and a suitable system architecture developed. The attractions of the area tactile sensor discussed here are its simplicity and low cost (in materials, construction, and required electronics).

Any material which is to be used should be thoroughly tested. Despite considerable recent research effort there seems to be no intrinsically conducting plastic or rubber material. Elastomers are made conducting by "loading" them with small conducting or semiconducting particles or coating them with a metallic film, with the result that resistivity, contact resistance, and changes of these with pressure, temperature and humidity may not be constant from batch to batch and over time. However, touch sensors need not be instrument grade transducers, and material properties should be considered in relation to actual requirements.

Material should be chosen with convenient elasticity, thickness, resistivity, contact resistance, and durability. The elastic properties of materials under and over the sensor can be very important in determining the sensor characteristics. Contact resistance may be a function of time: how does this affect a sensor's utility? A sensor should be easily and reproducibly made. This means that the basic material (conducting elastomer) should be available and consistent in both resistivity and contact resistance, and that leads should be easily attached, both to the edges of the plastic and to external circuitry. Design of a sensor should address all of these issues, as well as the installation on the robot hand.

One possible installation is to design the finger elements with leads internally wired to sockets which would accept a snap-in sensor module. The module itself might be designed so conducting membranes, "fleshy" layer, or protective surface layer could be easily changed: the outer human skin replaces itself every 20 to 30 days. All clamps and wires would be internal to the finger, so the final appearance would be a simple surface much as the Utah-MIT hand has now. The sockets might be designed to accept more than one type of sensor. Is would also be possible to build a socket designed to facilitate the installation of a sensor which would wrap around a finger element.

The amount of electrical noise which is present and may be tolerated should be determined experimentally before final installation plans are made. Currents appear to be sufficiently large that they may be brought away from the hand for measurement, although though this tends to increase capacitively and inductively coupled noise and places the resistance of the wires and various contact potentials in series with the sensor resistances. Alternatively, some circuitry might be placed in the finger or the hand, e.g., operational amplifiers to convert current to voltage while holding the input at (virtual) ground. Although more circuitry could be placed in the fingers, this would not reduce the number of required wires unless sensor output was multiplexed, since each sensor logically provides x and y locations and absolute magnitudes of x and y signals, all of which are useful. Input potential and ground (if needed by local circuitry) can be common for a number of sensors. At some point an A/D converter is needed, with enough channels for four per sensor (at most 60 for the hand); however, multiplexing and conversion circuitry can be small enough to fit in a finger [T88].

Software support at a minimum would make location and strength of contact available to any running program. A more interesting layer of software could exist just above this lowest level to combine sensory information into descriptions of object hardness, surface shape, and (perhaps) texture. This level would also monitor sensors at all times and correct for commonly occurring error conditions such as drift, hysteresis, or orientational effects, would automatically generate values for

calibration parameters after sensor elements were replaced, and would signal higher level processes to take needed corrective action ("there seems to be chewing gum stuck to the third finger").

Other sensors related to the basic sensor described above can be created. The simplest modification is to divide the electrodes of one or more sides into sections, each with a separate current lead to provide more information about the shape of the contact region at cost of additional wires. Linearity of position with output can be improved by placing resistors in series with the output currents, but this condition is difficult to handle theoretically; other modifications might include using curved electrodes or variable resistivity in the plane. Other sensors, featuring contact between the sides of thick interpenetrating electrodes in bar or circular patterns would allow a sensor to report shear forces, and perhaps also normal forces simultaneously. However, these sensors require that rather complicated structures be formed with elastic, deformable materials.

6. Conclusion

A new tactile sensor for robots has been described theoretically and demonstrated to have desirable traits through experiments with bench-top implementations. The sensor is novel in that the location of contact within the large sensor area is determined with arbitrary accuracy using only four wires per sensor (plus potential lead which may be common to many sensors). The primary advantages of the new sensor are sensitivity to light touch, ease of fabrication and use, and low cost. The largest problem in its development appears to be finding a suitable conducting elastomer, but there is active research in this area, many materials already exist, and combinations such as a conducting elastomer with a surface coating of a force sensitive resistive material can be considered. It seems important to equip dextrous manipulators with even crude touch sensors for research in manipulation to advance.

7. Acknowledgements

References

[3M]   Velostat electrically conductive bags, product 2004 of Static Control Systems Division/3M, Austin, TX 78769-2963.

[B84]   R.W. Brockett, "Robotic hands with rheological surfaces", *IEEE Robotics and Automation Conference* pp. 942-946 (1985).

[B88]   S. Begej, "Fingertip-shaped optical tactile sensor for robotic applications",
           IEEE Robotics and Automation Conference pp. 1752-1757, (1988).

[BF88]   R.S. Fearing and T.O. Binford, "Using a cylindrical tactile sensor for
           determining curvature", *IEEE Robotics and Automation Conference* pp.
           765-771 (1988).

[C75]   J.R. Cannon, "A class of inverse problems: the determination of second
           order elliptic partial differential operators from over-specified boundary
           data", in *Improperly posed boundary value problems*, A. Carasso and A.P.
           Stone, eds, Pitman Publishing, London, 1975.

[DD85]   P. Dario and D. De Rossi, "Tactile sensors and the gripping challenge",
           IEEE Spectrum **22** pp. 46-52, Aug. 1985.

[Dea85]   P. Dario, A. Bicchi, F. Vivaldi, P.C. Pinotti, "Tendon actuated explora-
           tory finger with polymeric, skin-like tactile sensor", *IEEE Robotics and
           Automation Conference* pp. 701-706, (1985).

[G78]   Many papers in *Active Touch*, G. Gordon, editor, Pergamon Press,
           Oxford, 1978.

[H80]   L.D. Harmon, "Touch sensing technology: a review", Technical report
           MSR 80-03, Soc. Manufacturing Engineers, Dearborn MI (1980).

[Ha82]   L.D. Harmon, "Automated tactile sensing", *The Intern. Journal of Robotics
           Research* **1** #2 pp. 3-32 (1982).

[Hi82]   W.D. Hillis "A high-resolution image touch sensor", *The Intern. Journal of
           Robotics Research* **1** #2 pp. 33-44 (1982).

[IE]   Interlink Electronics, Santa Barbara, CA 93103.

[J61]   L.B.W. Jolley, *Summation of Series*, second edition, Dover Publications,
           New York, 1961. Entry number 560.

[J62]   J.D. Jackson, *Classical Electrodynamics*, Wiley, New York, 1962.

[Jea88]   S. C. Jacobsen, I.D. McCammon, K.B. Biggers, and R. P. Phillips,
           "Design of tactile sensing systems for dextrous manipulators". *IEEE Con-
           trol Systems*, vol. 8 #1 pp. 3-13, (1988).

[K88]   R.J. Knops, reviewing *Ill-posed problems of mathematical physics and
           analysis*, Bulletin (new series) of the Am. Math. Soc. **19** pp. 332-337

(1988).

[M05]   H.F. Moulton, "Current flow in rectangular conductors", Proc. of the London Mathematical Society, series 2 vol. 3 pp. 104-110 (1905).

[RT82]   M.H. Raibert and J.E. Tanner, "Design and implementation of a VLSI tactile sensing computer", *The Intern. Journal of Robotics Research* **1** #3 pp. 3-18 (1982).

[RW83]   B.E. Robertson and A.J. Walkden, "Tactile sensor system for robotics", *SPIE Proceedings* **449**, pp. 572-577, (1983).

[SGH86] D. Siegel, I. Garabieta, J.M. Hollerbach, "An integrated tactile and thermal sensor", *IEEE Robotics and Automation Conference* pp. 1286-1291, (1986).

[SS78]   W.E. Snyder and J. St. Clair, "Conductive elastomers as sensor for industrial parts handling equipment", IEEE Trans. Instr. Measur. **IM-27** #1 pp. 94-99 (1978).

[T88]   B. Tise, "A compact high resolution piezoresistive digital tactile sensor", *IEEE Robotics and Automation Conference*, pp. 760-764, (1988).

[W75]   H. J. Woltring "Single- and dual-axis lateral photodetectors of rectangular shape", *IEEE Trans. Electron Devices* **ED-22** pp. 581-590 (1975).

8. Appendix A: Derivation of Equations of Theory section

Current flowing in a plane follows the gradient of the electric potential U, which itself is a solution of the two-dimensional Poisson equation

$$\nabla^2 U(x,y) = \frac{\partial^2 U}{\partial x^2} + \frac{\partial^2 U}{\partial y^2} = -\frac{\rho}{w} J(x,y), \tag{A1}$$

where ρ is the resistivity of the material, w is the thickness of the plane, and $J(x,y)$ is a spatially varying current source. The contact area can be modeled as a point source at (x_0,y_0) by using Dirac delta functions: $J(x,y) = J_0\delta(x-x_0)\delta(y-y_0)$. If the resistive plane occupies the rectangular region $0\leq x\leq a$ and $0\leq y\leq b$ the potential can be written as the Fourier expansion [J62]

$$U(x,y) = \frac{2}{\sqrt{ab}} \sum_{m=0}^{\infty} \sum_{n=0}^{\infty} A_{mn} \sin\frac{m\pi x}{a} \sin\frac{n\pi y}{b}. \tag{A2}$$

Coefficients of the cosine terms of this expansion are zero because $U=0$ on the boundaries of the plane. Substituting eq. A2 into eq. A1 yields

$$\frac{2}{\sqrt{ab}}\sum_{m,n} A_{mn}\left(\frac{m^2}{a^2}+\frac{n^2}{b^2}\right)\pi^2 \sin\frac{m\pi x}{a}\sin\frac{n\pi y}{b} = \frac{\rho J_0}{w}\delta(x-x_0)\delta(y-y_0), \tag{A3}$$

and the coefficients are determined in the usual manner:

$$A_{mn}\left(\frac{m^2}{a^2}+\frac{n^2}{b^2}\right)\pi^2 = \int_0^a\int_0^b\frac{2}{\sqrt{ab}}\sin\frac{m\pi x}{a}\sin\frac{n\pi y}{b}\frac{\rho J_0}{w}\delta(x-x_0)\delta(y-y_0)\,dx\,dy \tag{A4}$$

or

$$A_{mn} = \frac{2}{\pi^2\sqrt{ab}}\frac{\rho J_0}{w}\left(\frac{m^2}{a^2}+\frac{n^2}{b^2}\right)^{-1}\sin\frac{m\pi x_0}{a}\sin\frac{n\pi y_0}{b}. \tag{A5}$$

Thus the electric potential at any point on the rectangle is

$$U(x,y) = \frac{4\rho J_0}{\pi^2 abw}\sum_{m=1}^{\infty}\sum_{n=1}^{\infty}\left(\frac{m^2}{a^2}+\frac{n^2}{b^2}\right)^{-1}\sin\frac{m\pi x_0}{a}\sin\frac{n\pi y_0}{b}\sin\frac{m\pi x}{a}\sin\frac{n\pi y}{b}. \tag{A6}$$

The current flowing across a small element can be determined by noting that the potential difference across the element is both the gradient of the potential at that element and the product of the resistance of the element and the current traversing it. The current exiting a side is simply the sum of currents crossing all elements which compose the side, and as the elements become infinitesimal this sum becomes an integral. For example, the current which leaves the side at $x=0$ is (since current flows against the gradient)

$$I_{x=0} = -\int_{y=0}^{b}\left[\frac{w}{\rho}\frac{\partial U}{\partial x}\right]_{x=0}dy. \tag{A7}$$

Using eq. A6 for U(x,y) and simplifying leads to

$$I_{x=0} = \frac{8J_0}{ab\pi^2} \sum_{m=1}^{\infty} \sum_{n=1}^{\infty} \frac{\dfrac{m}{2n-1}\dfrac{b}{a}}{\left[\dfrac{m^2}{a^2} + \dfrac{(2n-1)^2}{b^2}\right]} \sin\frac{m\pi x_0}{a} \sin\frac{(2n-1)\pi y_0}{b} \quad . \tag{A8}$$

The $(2n-1)$ factor results from the difference of $\cos n\pi y/b$ evaluated at $y=b$ and $y=0$, which is -2 or 0 depending on whether the original n is odd or even. Only odd terms survive in the original sum.

Although the sums in eq. A8 need not be extended to infinity, n and m must both go to several hundred for reasonable accuracy. Numerical accuracy is easily checked since the sum of all currents must equal the injected current J_0. Deviations on the order of 1% were observed with both indices going to 199; with indices going to 531 the average deviation for 15 locations was about 0.1%, although total current was 0.6% high for $x=0.9a$, $y=0.9b$. Computation for these 15 points required several hours on a VAX 785.

Computation time can be greatly reduced by eliminating one summation using [J61]

$$\sum_{m=1}^{\infty} \frac{m \sin(m\theta)}{m^2 + \phi^2} = \frac{\pi}{2} \frac{\sinh\phi(\pi-\theta)}{\sinh\pi\phi} \quad . \tag{A9}$$

Re-writing eq. A8 to bring it into this form and identifying θ as $\pi x_0/a$ and ϕ as $(2n-1)a/b$ yields

$$I_{x=0} = \frac{4J_0}{\pi} \sum_{n=1}^{\infty} \frac{\sin[(2n-1)\pi y_0/b]}{2n-1} \frac{\sinh[(2n-1)\pi(a-x_0)/b]}{\sinh[(2n-1)\pi a/b]} \quad . \tag{A10}$$

Currents for the side at $x=a$ can be written down immediately using symmetry from eq. A10:

$$I_{x=a} = \frac{4J_0}{\pi} \sum_{n=1}^{\infty} \frac{\sin[(2n-1)\pi y_0/b]}{2n-1} \frac{\sinh[(2n-1)\pi x_0/b]}{\sinh[(2n-1)\pi a/b]} , \tag{A11}$$

and similar equations result for the top and bottom currents by interchanging a and b, m and n, and x and y.

Currents computed using these expressions converge very rapidly; summing only the first 10 terms yielded a total current within 0.01% of J_0 for x and y values between 0.1 and 0.9 of full scale. This rapid convergence (for $I_{x=a}$) is due to the behavior of the second factor, which can be written as $\sinh(vx_0/a) / \sinh v$, where $v \equiv (2n-1)\pi a/b$.

$$\frac{\sinh(vx_0/a)}{\sinh v} = \frac{e^{vx_0/a} - e^{-vx_0/a}}{e^v - e^{-v}} \approx e^{-\frac{v}{a}(a-x_0)} = e^{-(2n-1)\pi(a-x_0)/b}. \tag{A12}$$

This form is also important because it makes it possible to bring out the predominant dependence of the current on the source location, and will make it possible to invert the equation to give the approximate location as a function of currents. Eq. A11 can be re-written as

$$I_{x=a} = \frac{4J_0}{\pi} \sum \sin\frac{(2n-1)\pi y_0}{b} \frac{e^{-(2n-1)\pi(a-x_0)/b}}{2n-1} \tag{A13}$$

which expands to

$$I_{x=a} = \frac{4J_0}{\pi} e^{-\pi(a-x_0)/b} \left[\sin\pi y_0/b + \frac{e^{-2\pi(a-x_0)/b}\sin 3\pi y_0/b}{3} + \cdots \right] \tag{A14}$$

Similarly,

$$I_{x=0} = \frac{4J_0}{\pi} e^{-\pi x_0/b} \left[\sin\pi y_0/b + \frac{e^{-2\pi x_0/b}\sin 3\pi y_0/b}{3} + \cdots \right] \tag{A15}$$

The ratio of the two currents

$$\frac{I_{x=a}}{I_{x=0}} \approx \frac{e^{-\pi(a-x_0)/b}}{e^{-\pi x_0/b}} = e^{2\pi(x_0-a/2)/b}. \tag{A16}$$

This allows us to define an observed position defined as

$$x_{obs} = \frac{a}{2} + \frac{b}{2\pi} \log\frac{I_{x=a}}{I_{x=0}} \tag{A17}$$

$$y_{obs} = \frac{b}{2} + \frac{a}{2\pi} \log\frac{I_{y=b}}{I_{y=0}}.$$

The equations of section 3.1 follow the above development exactly, and all equations of that section appear here in identical form. In the following the development of section 3.2 is carried out with intermediate steps filled in.

Consider a rod of high conductivity held at potential V^+ which is pressed against the center of a circular planar resistor. The rod has radius A, the planar resistor has radius B, resistivity ρ, and thickness w (thus ρ/w ohms/square), and its circumference is held at potential 0 (ground). Current from the cylindrical electrode passes through a uniform (surface) resistive layer of $\sigma/\pi A^2$ ohms. From symmetry, current flows radially within the plane, and current at $r=0$ is zero; let $I(r)$ represent the current crossing a cylindrical surface at radius r.

Detailed consideration allows a functional form for $I(r)$ to be determined. The current which enters the annular volume at r is

$$I(r+\delta r) - I(r) = \frac{V^+ - V(r)}{\sigma} 2\pi r \delta r , \tag{A18}$$

which can be rewritten as

$$V(r) = V^+ - \frac{\sigma}{2\pi r} \frac{dI(r)}{dr} . \tag{A19}$$

$2\pi r\delta r$ represents the area of contact of the annular volume with the electrode. Potential $V(r)$ in the resistive plane is due exclusively to current flow to ground. From the change in voltage across a small annulus

$$\delta V = \frac{-\rho I(r)}{2\pi w r}\delta r \tag{A20}$$

an expression for the potential can be derived:

$$V(r) = V_A - \int_A^r \frac{\rho I(r) dr}{2\pi w r} \tag{A21}$$

where V_A is the potential at $r = A$. Eqs. A19 and A21 together yield

$$V^+ - V_A - \frac{\sigma}{2\pi} \frac{dI}{r dr} + \frac{\rho}{2\pi w} \int_A^r \frac{I(r) dr}{r} = 0 . \tag{A22}$$

A solution for $I(r)$ can be found by substituting the expansion

$$I(r) = \sum_{n=1}^{\infty} a_m (r/A)^n \tag{A23}$$

into eq. A22 and equating powers of r. From the coefficients of r^{-1} follows $a_1 = 0$. The constant terms yield

$$V^+ - V_A - \frac{\sigma}{2\pi} \frac{2a_2}{A^2} - \frac{\rho}{2\pi w} \sum \frac{a_n}{n} = 0 . \tag{A24}$$

For all higher powers the $n + 2$nd coefficient is related to the nth by

$$a_{n+2} = \frac{\rho A^2}{w\sigma} \frac{a_n}{(n+2)n} . \tag{A25}$$

Thus all odd powers have zero coefficients, and (after some rearranging)

$$I(r) = a_2 \sum_{m=1}^{\infty} \left[\frac{\rho A^2}{4w\sigma} \right]^{m-1} \frac{1}{m!(m-1)!} \left[\frac{r}{A} \right]^{2m} . \tag{A26}$$

Eq. A24 determines a_2, using

$$\sum \frac{a_n}{n} = a_2 \sum_{m=1}^{\infty} \left[\frac{\rho A^2}{4w\sigma} \right]^{m-1} \frac{1}{(2m)m!(m-1)!} \tag{A27}$$

and

$$V_A = I(A) R_p = a_2 R_p \sum_{m=1}^{\infty} \left[\frac{\rho A^2}{4w\sigma} \right]^{m-1} \frac{1}{m!(m-1)!} . \tag{A28}$$

Note that $I(A)$ is simply the total current that flows in the plane. R_p, the resistance of the plane, can be calculated from the sum of series resistances across infinitesimal annular volumes which the current traverses from $r = A$ to $r = B$:

$$R_p = \int_A^B \frac{\rho dr}{2\pi r w} = \frac{\rho}{2\pi w} \log(B/A) . \tag{A29}$$

This same result obtains in the case of concentric squares of sides A and B [M05]. After some algebra,

$$a_2 = \frac{V^+}{\dfrac{\sigma}{\pi A^2} + \dfrac{\rho}{4\pi w} \sum_{m=1}^{\infty} \left[\dfrac{\rho A^2}{4w\sigma} \right]^{m-1} \dfrac{[2\log(B/A) + 1/m]}{m!(m-1)!}} . \tag{A30}$$

The total current is, from eqs. A26 and A30,

$$I(A) = \cfrac{V^{+} \displaystyle\sum_{m=1}^{\infty} \left[\dfrac{\rho A^2}{4w\sigma}\right]^{m-1} \dfrac{1}{m!(m-1)!}}{\dfrac{\sigma}{\pi A^2} + \dfrac{\rho}{4\pi w} \displaystyle\sum_{m=1}^{\infty} \left[\dfrac{\rho A^2}{4w\sigma}\right]^{m-1} \dfrac{[2\log(B/A)+1/m]}{m!(m-1)!}} \ . \qquad \text{(A31)}$$
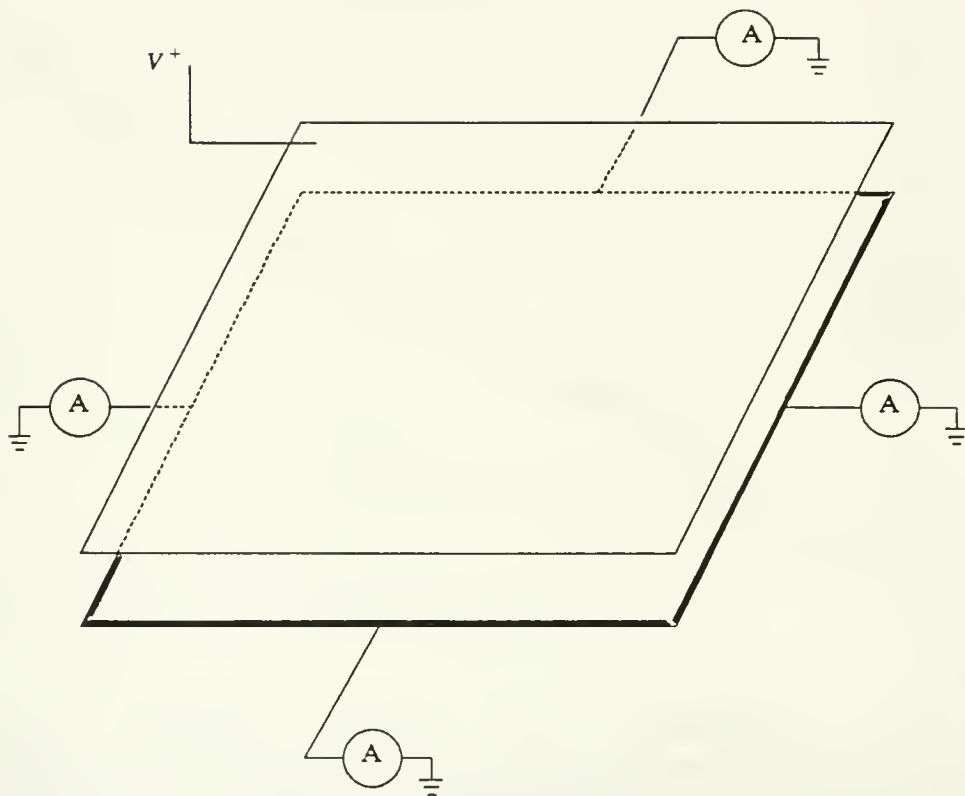
Fig. 1. Sketch of a planar touch sensor. Upper conducting membrane is held at potential V^+, and current is collected from electrodes of excellent conductivity along the four sides of the poorly conducting plane. Pressure on a small region of the upper membrane brings it into contact with the lower and allows current to flow. Vertical scale is greatly exaggerated.
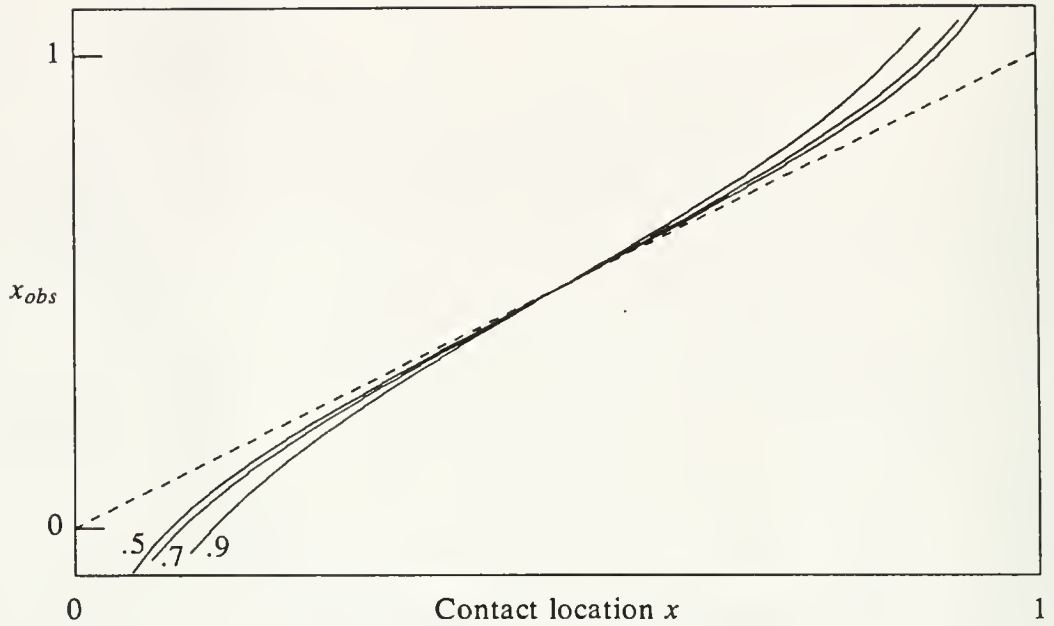
Fig. 2. Dependence of observed position, defined as $x_{obs} = .5 + (1/2\pi) \, log \, (I_{x=1}/I_{x=0})$, on the position of contact within the unit square sensor. Solid curves are theoretical results for 3 values of y: .5 (vertical center-line), .7, and .9; currents were computed using eqs. 4 and 5. Dashed line shows $x_{obs} = x$.
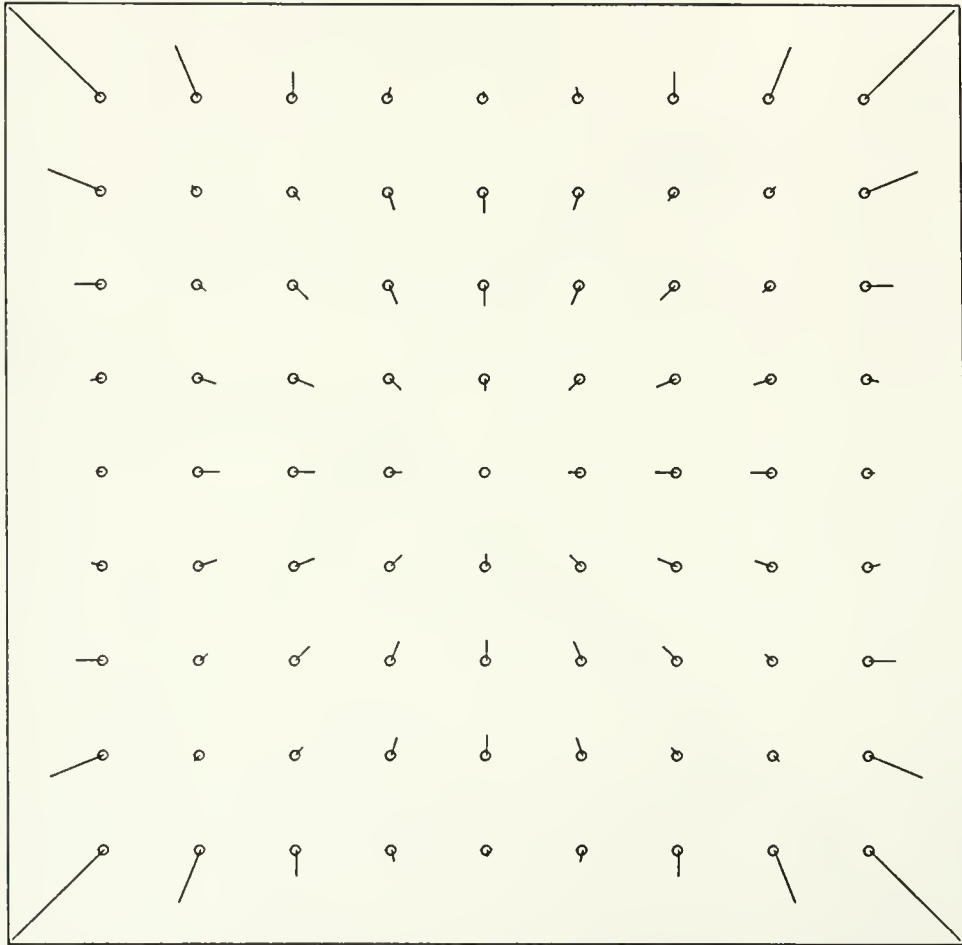
Fig. 3. Error as a function of position for a linearized square sensor. Square indicates the sensor area, circles a grid of true locations, and the lines show the displacement from a grid point to its sensed location. The coefficient of the log terms (eq. 8) has been adjusted so all grid points from x or y = .1 to .9 will appear to be within the sensor area. For accurate work these deviations can be avoided by using correction functions or look-up tables.
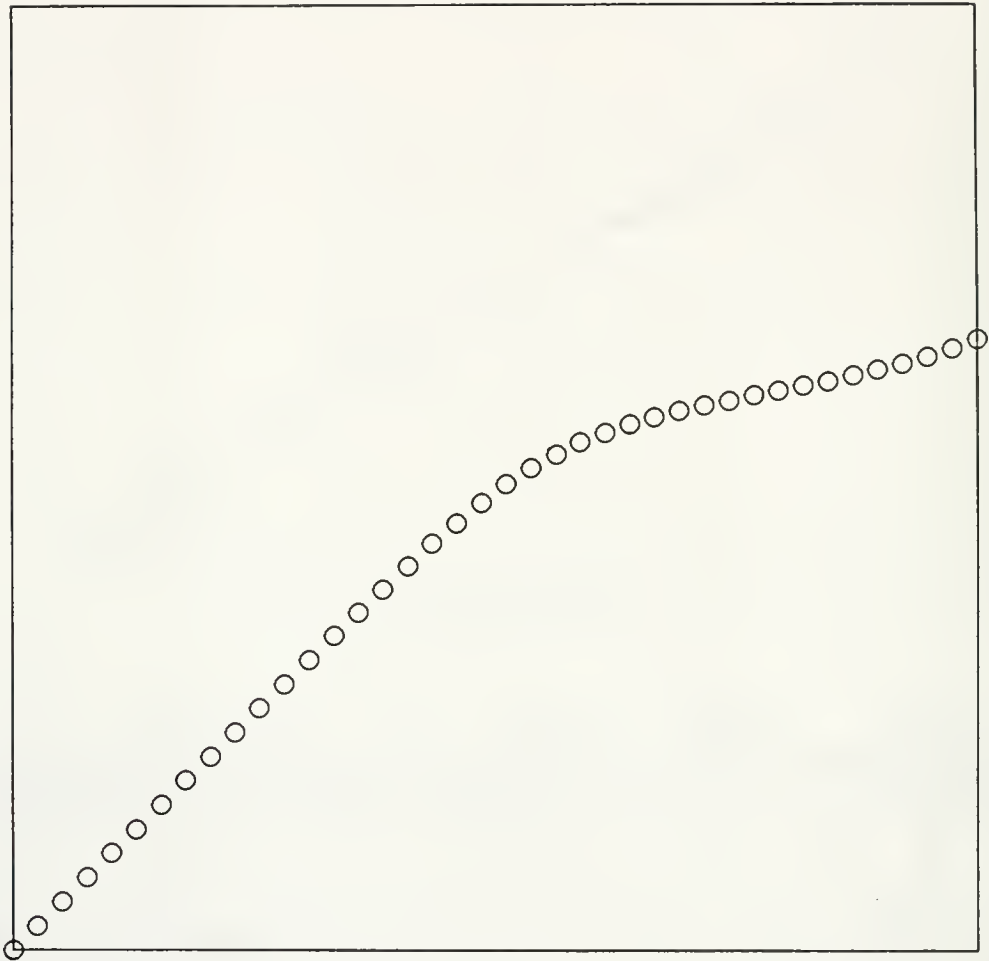
Fig. 4. Log-log plot of current vs contact area. Vertical and horizontal scales are the same. Radius of the electrode A varies by a factor of 10,000, and is 0.4 B at its largest value.
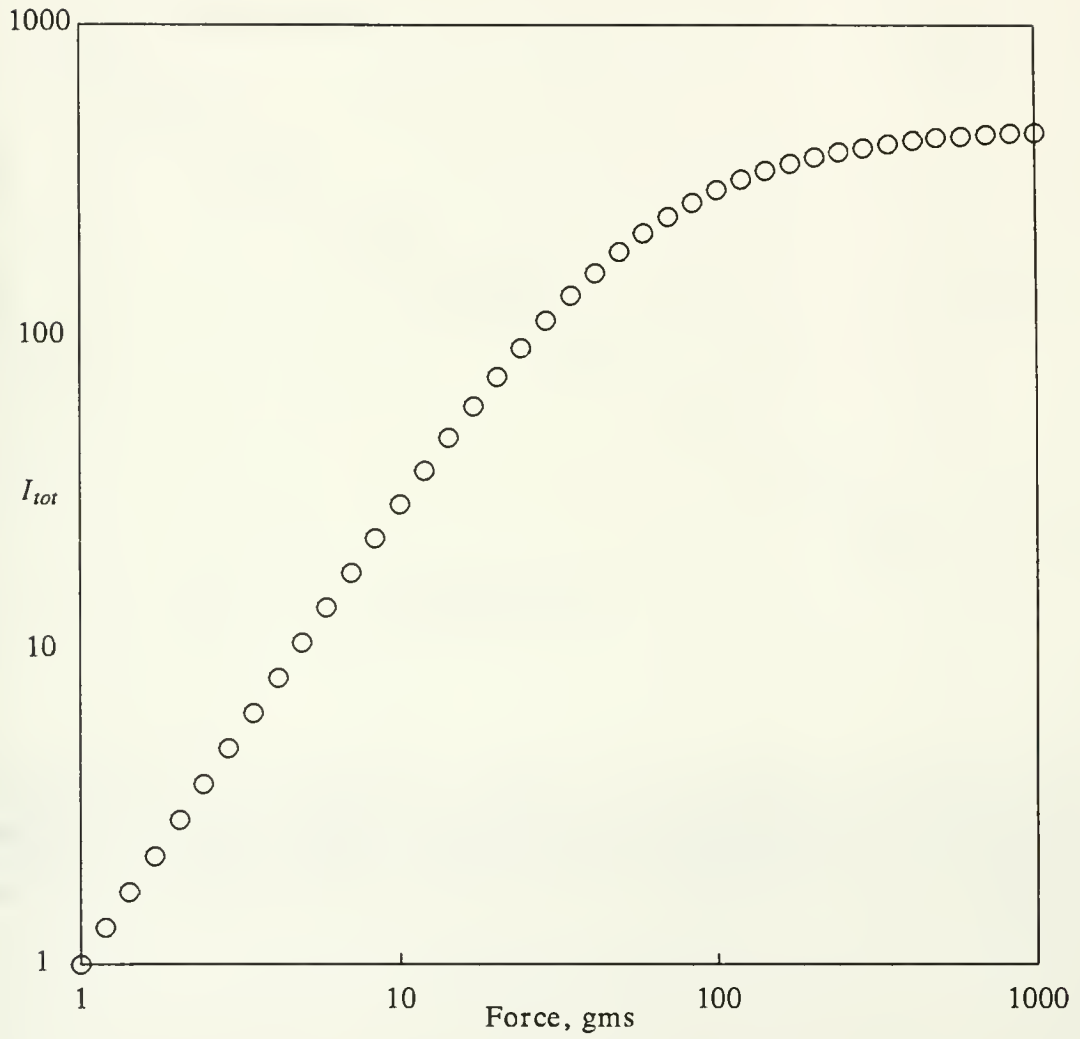
Fig. 5. Log-log plot of total current vs contact force for constant area calculated from eqs. 11 and 12 for $\alpha = 1.5$. Current is in arbitrary units.
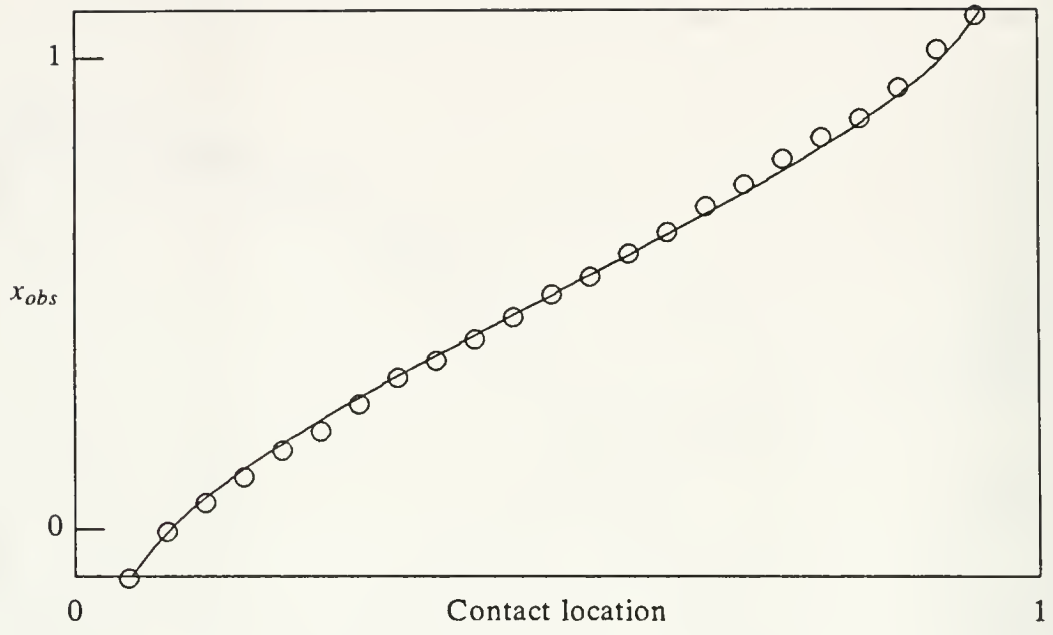
Fig. 6. Observed location vs true location for points along the centerline of a square piece of conducting plastic with electrodes along the edges. x_{obs} is defined as in fig. 2; the circles represent measured currents and the solid line is a theoretical plot, as in fig. 1. The data has not been scaled in any way to fit the theoretical curve.
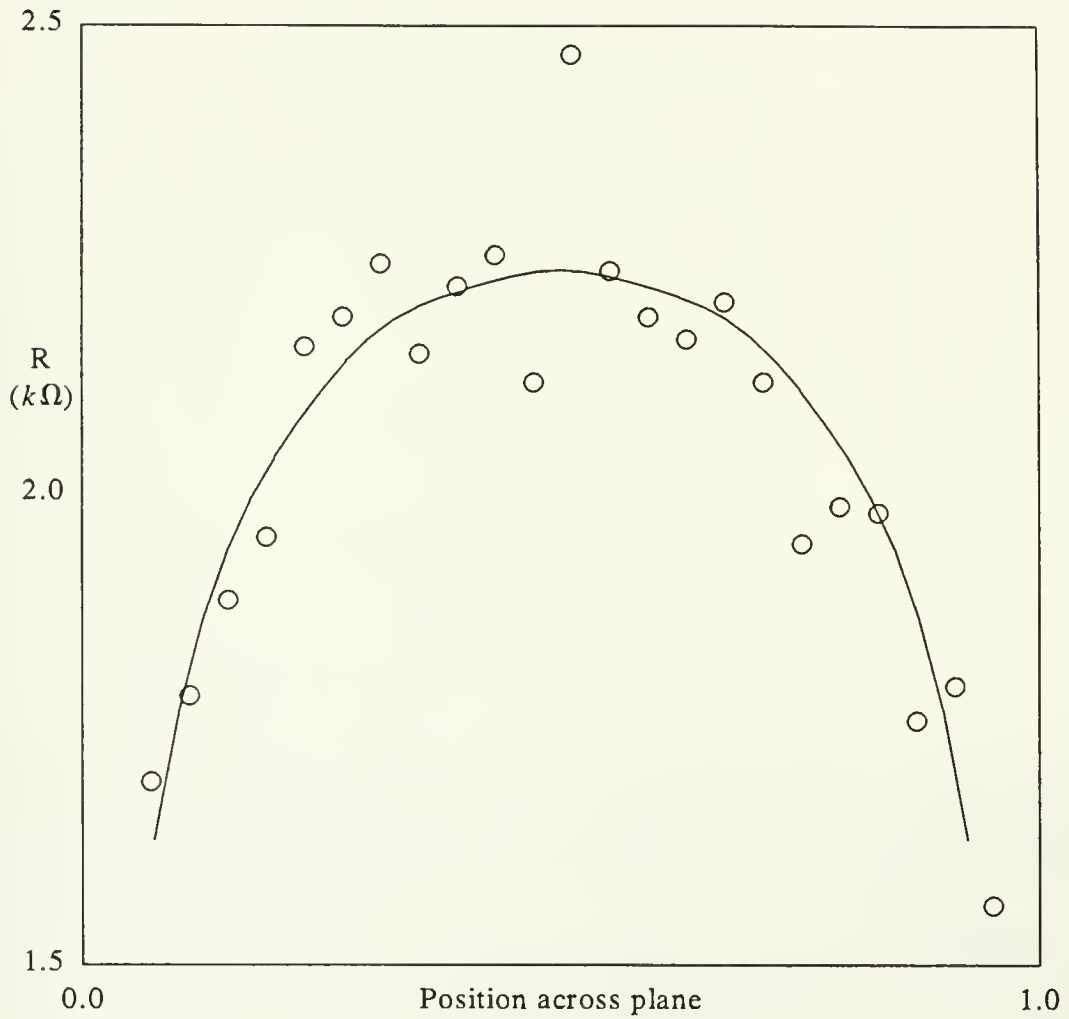
Fig. 7. Resistance of the plane ($k\Omega$) vs location along the mid-line of a square of conducting plastic with electrodes along the edges. Circles represent measurements; the large scatter is due primarily to variations in the contact resistance. Solid curve is theoretical result (see text).
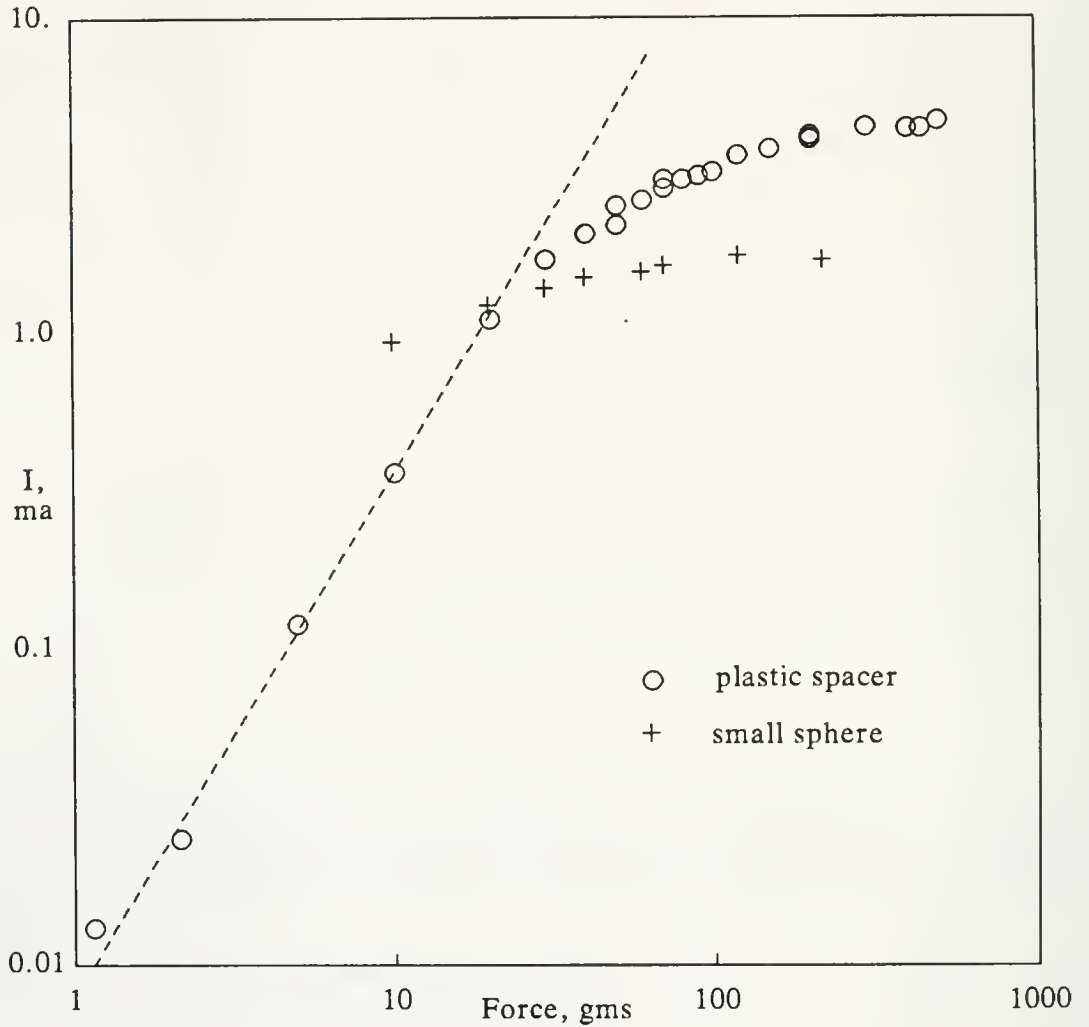
Fig. 8. Experimental total current vs contact force for prototype sensor S1 for two different objects, a plastic spacer about 1 cm square and a sphere of about 0.8 cm radius. Error bars on the points below 5 gms are quite large. Dashed line has a slope of 1.57 on this log-log plot. Cf. fig. 5.
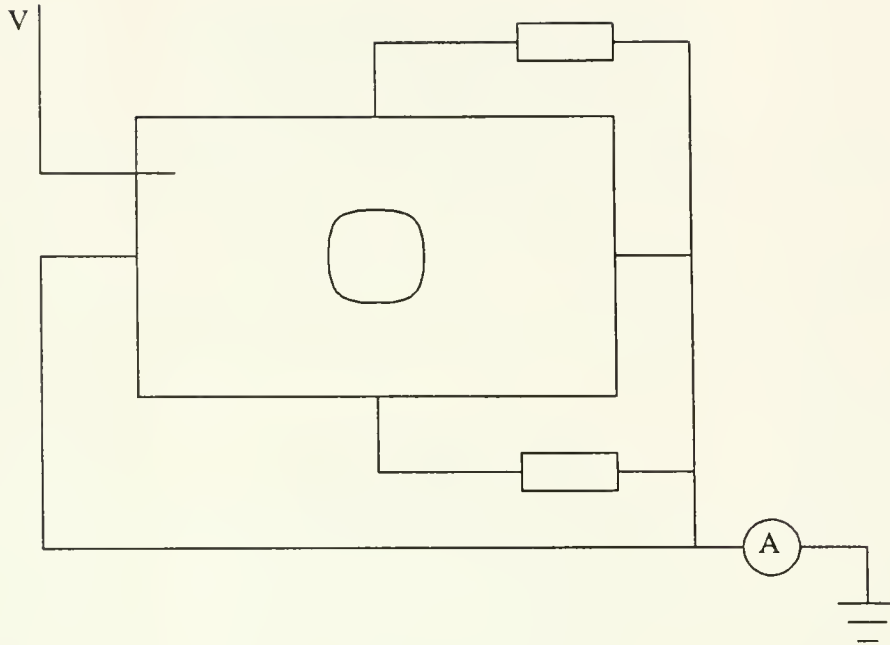
Fig. 9. Sensor and circuit to measure total current during repetitive tests. Rectangle represents a double layer sensor as in fig. 1; force is applied to a plastic spacer in the center. Resistors, 336 Ω for S1 and 5600 Ω for S2, reduce the sensitivity to small changes in the position of the spacer. V was 12 volts; current was measured using a digital multimeter.

DATE DUE	BORROWER'S NAME

This book may be kept **SEP 3 0 1988**
FOURTEEN DAYS
A fine will be charged for each day the book is kept overtime.

GAYLORD 142   PRINTED IN U.S.A.